Journal of Guidance, Control, and Dynamics, Vol. 42, No. 2, 2019, pp. 411–415. doi: http://doi.org/10.2514/1.G003900

Elliptic Displaced Orbit Approximation with Equally Spaced Impulses

Andrea Caruso,* Giovanni Mengali,† and Alessandro A. Quarta‡
Department of Civil and Industrial Engineering, University of Pisa, I-56122 Pisa, Italy

Nomenclature

B	=	virtual body
$\overrightarrow{BP}$	=	position vector of point P in $\mathcal{T}$, km
e	=	reference orbit eccentricity
H	=	displacement distance, km
$\hat{\boldsymbol{\imath}}, \hat{\boldsymbol{\jmath}}, \hat{\boldsymbol{k}}$	=	unit vectors of $\mathcal{T}$
$\hat{\boldsymbol{\imath}}_I, \hat{\boldsymbol{\jmath}}_I, \hat{\boldsymbol{k}}_I$	=	unit vectors of $\mathcal{T}_I$
N	=	number of impulsive maneuvers per revolution
O	=	primary body center-of-mass
$\overrightarrow{OP}$	=	position vector of point P in $\mathcal{T}_I$, km
P	=	maneuver point
$\mathcal{P}$	=	DNKO plane
p	=	reference orbit semilatus rectum, km
$\boldsymbol{r}$	=	relative position vector, km
$\mathcal{T}$	=	orbital reference frame
$\mathcal{T}_I$	=	inertial reference frame
$\boldsymbol{v}$	=	relative velocity vector, km/s
x, y, z	=	components of $\boldsymbol{r}$ in $\mathcal{T}$, km
$\Delta\boldsymbol{v}$	=	velocity variation vector, m/s
Δv	=	total velocity variation per revolution, m/s
$\Delta\nu$	=	true anomaly variation within each arc, rad
μ	=	primary body gravitational parameter, $\mathrm{km}^3/\mathrm{s}^2$
ν	=	true anomaly, rad
$\boldsymbol{\omega}$	=	angular velocity vector, rad/s

Subscripts

c	=	continuous thrust case
e	=	end of ballistic arc
i	=	i-th ballistic arc or impulsive maneuver
max	=	maximum value
s	=	start of ballistic arc
$\oplus$	=	Earth
$\odot$	=	Sun

Superscripts

$\dot{}$	=	time derivative
$'$	=	derivative with respect to ν
$\sim$	=	transformed variable

Introduction

A displaced non-Keplerian orbit (DNKO) is a closed, two-dimensional, trajectory whose orbital plane does not contain the primary body center-of-mass, and is maintained by a continuous thrust that balances the centrifugal and gravitational forces acting on the spacecraft [1, 2]. Since the pioneering work of Forward [3–5], DNKOs have been extensively studied in both geocentric [6–8] and heliocentric [9, 10] mission scenarios. In principle, a DNKO can be approximated with a sequence of Keplerian arcs patched by impulsive maneuvers, so that the points where the impulses are applied coincide with points belonging to the original DNKO [11, 12]. Such a trajectory type, which will be referred to as closed patched orbit (CPO), has been thoroughly investigated by McInnes [13], who proposed an elegant mathematical model useful for approximating DNKOs of circular shape.

The aim of this Note is to extend the results of Ref. [13] to the case of two-body elliptic DNKOs, by obtaining a general method to calculate the propulsive performance of a spacecraft that covers the corresponding CPOs. In particular, the proposed approach gives the analytical expression of the total velocity variation per revolution around the primary body, required to approximate an assigned DNKO with a sequence of (azimuthally) equally spaced impulsive maneuvers. The value of the total velocity variation in the continuous thrust scenario is also obtained as a special case of the mathematical model.

*Ph.D. student, andrea.caruso@ing.unipi.it
†Professor, g.mengali@ing.unipi.it. Senior Member AIAA.
‡Professor, a.quarta@ing.unipi.it. Associate Fellow AIAA (**corresponding author**).

To this end, the spacecraft motion along the CPO is investigated using the linearized Hill-Clohessy-Wiltshire equations for elliptic orbits [14], which describe the relative motion between the spacecraft and a virtual body that follows a reference (elliptic) Keplerian trajectory obtained by setting the DNKO displacement equal to zero. The only limitation of the proposed method is in the assumption of a small distance between the virtual body and the spacecraft, which, in its turn, implies a sufficiently small value of DNKO displacement. A nonlinear numerical simulation of the problem, obtained by solving a series of targeting problems, shows that the proposed set of equations gives an accurate approximation of the actual total velocity variation per revolution.

Problem description

Consider a virtual body B in a reference elliptic (Keplerian) orbit of semilatus rectum p and eccentricity $e < 1$, which moves around a primary body of gravitational parameter μ and center-of-mass O. Let $\nu \in [0,\, 2\pi]$ rad be the true anomaly of B, and $\boldsymbol{\omega}$ its angular velocity, with $\|\boldsymbol{\omega}\| = \dot{\nu}$. Introduce an inertial reference frame $\mathcal{T}_I$ with origin at O and unit vectors $\{\hat{\boldsymbol{\imath}}_I, \hat{\boldsymbol{\jmath}}_I, \hat{\boldsymbol{k}}_I\}$ with $\hat{\boldsymbol{k}}_I \equiv \boldsymbol{\omega}/\dot{\nu}$, and an orbital reference frame $\mathcal{T}$ with origin at B and unit vectors $\{\hat{\boldsymbol{\imath}}, \hat{\boldsymbol{\jmath}}, \hat{\boldsymbol{k}}\}$ with $\hat{\boldsymbol{\jmath}} = -\hat{\boldsymbol{k}}_I$. The plane $(\hat{\boldsymbol{\imath}}_I, \hat{\boldsymbol{\jmath}}_I) \equiv (\hat{\boldsymbol{\imath}}, \hat{\boldsymbol{k}})$ contains the reference orbit whose pericenter belongs to the direction of $\hat{\boldsymbol{\imath}}_I$, and $\hat{\boldsymbol{k}}$ points towards O, see Fig. 1.

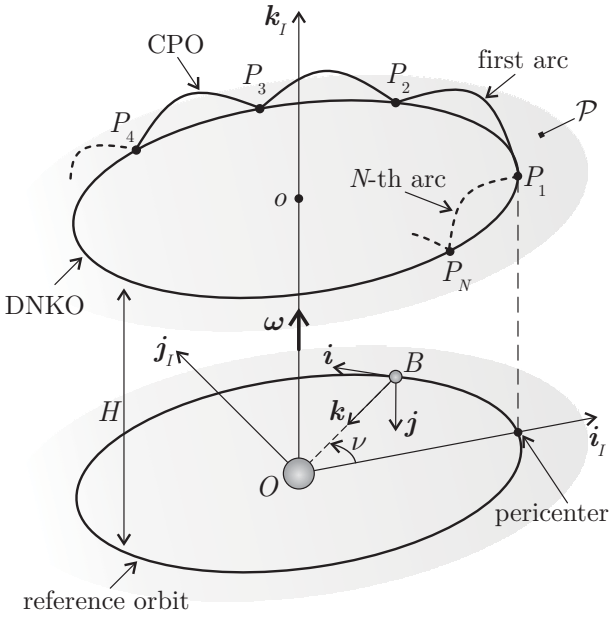

Figure 1 Reference frames.

Consider now a DNKO obtained by moving the reference orbit by a given distance H with a translation (without rotation) along the positive direction of $\hat{\boldsymbol{k}}_I$. The orthogonal projection of O on the plane $\mathcal{P}$ of the DNKO, which coincides with the focus of the displaced ellipse, is denoted by o. Let $\{P_1, P_2, \ldots, P_N\}$, with $N \geq 3$, be a set of angularly equally spaced points along the DNKO, so that the generic point P_i (with $i = 1, 2, \ldots, N$) coincides with the projection of B on the plane $\mathcal{P}$ when the true anomaly of the virtual body is $\nu = \nu_i$, where

$$\nu_i = (i-1)\Delta\nu \qquad \text{with} \qquad \Delta\nu \triangleq \frac{2\,\pi}{N} \tag{1}$$

Since $\nu_1 = 0$, P_1 is the DNKO pericenter, whereas the assumption of $N \geq 3$ implies that $\Delta\nu \leq 2\pi/3$. The position vector of the generic point P_i in the inertial reference frame $\mathcal{T}_I$ is given by

$$\overrightarrow{OP}_i = \cos\nu_i\,\hat{\boldsymbol{\imath}}_I + \sin\nu_i\,\hat{\boldsymbol{\jmath}}_I + H\,\hat{\boldsymbol{k}}_I \tag{2}$$

while the position vector of P_i in the orbital reference frame $\mathcal{T}$ is

$$\overrightarrow{BP}_i = -H\,\hat{\boldsymbol{\jmath}} \tag{3}$$

The given DNKO is approximated by a CPO, made up of a sequence of N ballistic arcs, each one starting at P_i and ending at P_{i+1}, and N impulsive maneuvers, each one occurring at the generic point P_i [13], see Fig. 1. The problem is to find the total velocity variation per revolution around the primary body Δv, required to maintain the CPO. In particular, a spacecraft S that follows the CPO intersects the DNKO at points P_i where the vehicle reaches its minimum distance (equal to H) from the $(\hat{\boldsymbol{\imath}}_I, \hat{\boldsymbol{\jmath}}_I)$ plane. In the limit as $N \to \infty$, the spacecraft S maintains a constant distance H from the $(\hat{\boldsymbol{\imath}}_I, \hat{\boldsymbol{\jmath}}_I)$ plane. In that case, the CPO coincides with the DNKO, and the multiple impulse analysis gives the same results (that is, the same Δv) as the continuous thrust case.

Mathematical model

The value of Δv can be obtained by analyzing the motion of S relative to B from $\nu = \nu_i$ to $\nu = \nu_i + \Delta\nu$ (that is, in the generic i-th ballistic arc), where $\{\nu_i, \Delta\nu\}$ are given by Eq. (1) as a function of the given number N of impulsive maneuvers.

Note that, at the beginning (or at the end) of i-th ballistic arc, the spacecraft position coincides with point P_i (or $P_{(i+1)}$), which belongs to the y-axis at a distance H from B, see Eq. (3).

Paralleling the procedure described by Yamanaka and Ankersen [14], when the distance between B and S is small compared to the distance between O and B, that is, when the spacecraft is close to the DNKO and the displacement H is sufficiently small, the motion of S relative to B in the i-th ballistic arc is approximated by the following set of linear differential equations

$$\ddot{x} = -k\sqrt{\dot{\nu}^3}\,x + 2\,\dot{\nu}\,\dot{z} + \ddot{\nu}\,z + \dot{\nu}^2\,x \tag{4}$$

$$\ddot{y} = -k\sqrt{\dot{\nu}^3}\,y \tag{5}$$

$$\ddot{z} = 2\,k\sqrt{\dot{\nu}^3}\,z - 2\,\dot{\nu}\,\dot{x} - \ddot{\nu}\,x + \dot{\nu}^2 z \tag{6}$$

where

$$k \triangleq \sqrt[4]{\frac{\mu}{p^3}} \tag{7}$$

is a constant parameter that depends on the semilatus rectum of the reference orbit, and $\{x, y, z\}$ are the components of the (relative) position vector $\boldsymbol{r} \triangleq \overrightarrow{OS} - \overrightarrow{OB}$ in the orbital reference frame $\mathcal{T}$, see Fig. 2, viz.

$$\boldsymbol{r} = x\,\hat{\boldsymbol{i}} + y\,\hat{\boldsymbol{j}} + z\,\hat{\boldsymbol{k}} \tag{8}$$

Using the true anomaly $\nu \in [\nu_i,\, \nu_i + \Delta\nu]$ as independent variable and introducing the transformation

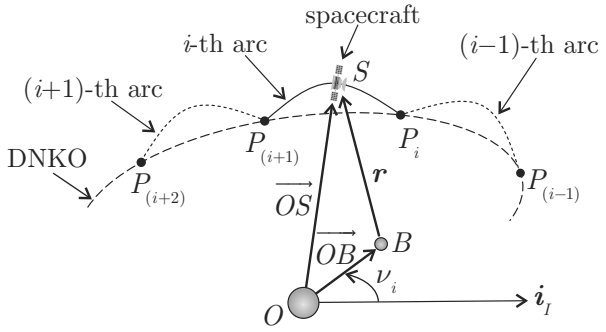

Figure 2 Relative position vector.

$$\widetilde{x} \triangleq \rho\,x \quad , \quad \widetilde{y} \triangleq \rho\,y \quad , \quad \widetilde{z} \triangleq \rho\,z \qquad \text{with} \qquad \rho \triangleq 1 + e\,\cos\nu \tag{9}$$

the linearized equations of relative motion Eqs. (4)–(6) reduce to [14]

$$\widetilde{x}'' = 2\,\widetilde{z}' \tag{10}$$

$$\widetilde{y}'' = -\widetilde{y} \tag{11}$$

$$\widetilde{z}'' = \frac{3\,\widetilde{z}}{\rho} - 2\,\widetilde{x}' \tag{12}$$

where the prime symbol denotes a derivative with respect to ν. The velocity vector of S relative to B, that is, $\boldsymbol{v} \triangleq \dot{\boldsymbol{r}}$, is [14]

$$\boldsymbol{v} = k^2\,\left(e\,\sin\nu\,\widetilde{\boldsymbol{r}} + \rho\,\widetilde{\boldsymbol{v}}\right) \tag{13}$$

where k is given by Eq. (7), and $\{\widetilde{\boldsymbol{r}}, \widetilde{\boldsymbol{v}}\}$ are defined as

$$\widetilde{\boldsymbol{r}} = \rho\,\boldsymbol{r} \equiv \widetilde{x}\,\hat{\boldsymbol{i}} + \widetilde{y}\,\hat{\boldsymbol{j}} + \widetilde{z}\,\hat{\boldsymbol{k}} \qquad , \qquad \widetilde{\boldsymbol{v}} = \widetilde{x}'\,\hat{\boldsymbol{i}} + \widetilde{y}'\,\hat{\boldsymbol{j}} + \widetilde{z}'\,\hat{\boldsymbol{k}} \tag{14}$$

From Eqs. (10) and (12), the spacecraft motion in the plane (x, z) can be represented in a compact form as

$$\left[\widetilde{x}(\nu),\, \widetilde{z}(\nu),\, \widetilde{x}'(\nu), \widetilde{z}'(\nu)\right]^{\mathrm{T}} = \Phi\,\left[\widetilde{x}(\nu_i),\, \widetilde{z}(\nu_i),\, \widetilde{x}'(\nu_i), \widetilde{z}'(\nu_i)\right]^{\mathrm{T}} \tag{15}$$

where $\Phi = \Phi(e, \nu) \in \mathbb{R}^{(4\times4)}$ is the state transition matrix, whose entries are detailed in Ref. [14]. Also, from Eq. (11), the motion of S along the y-axis is a free harmonic oscillation, that is

$$\widetilde{y}(\nu) = \widetilde{y}'(\nu_i)\,\sin\left(\nu - \nu_i\right) + \widetilde{y}(\nu_i)\,\cos\left(\nu - \nu_i\right) \tag{16}$$

$$\widetilde{y}'(\nu) = \widetilde{y}'(\nu_i)\,\cos\left(\nu - \nu_i\right) - \widetilde{y}(\nu_i)\,\sin\left(\nu - \nu_i\right) \tag{17}$$

Note that at both the beginning and the end of the i-th ballistic arc the spacecraft S lies in the y-axis, see Eq. (3), or

$$\widetilde{x}(\nu_i) = \widetilde{z}(\nu_i) = \widetilde{x}(\nu_i + \Delta\nu) = \widetilde{z}(\nu_i + \Delta\nu) = 0 \tag{18}$$

Therefore, from Eq. (15), it follows that $\widetilde{x}'(\nu_i) = \widetilde{z}'(\nu_i) = 0$, that is

$$\widetilde{x}(\nu) = \widetilde{z}(\nu) = \widetilde{x}'(\nu) = \widetilde{z}'(\nu) = 0 \tag{19}$$

As a result, with the approximation of Eqs. (10)–(12), the spacecraft motion only evolves along the (negative) y-axis of the orbital reference frame according to Eqs. (16)–(17).

Bearing in mind that $y(\nu_i) = y(\nu_i + \Delta\nu) = -H$, the following constraints are obtained from the second of Eqs. (9)

$$\frac{\widetilde{y}(\nu_i)}{1 + e\,\cos\nu_i} = \frac{\widetilde{y}(\nu_i + \Delta\nu)}{1 + e\,\cos\left(\nu_i + \Delta\nu\right)} = -H \tag{20}$$

Combining Eq. (16) with (20), the expression of $\widetilde{y}'(\nu_i)$ is

$$\widetilde{y}'(\nu_i) = \frac{H\,\left(e\,\sin\Delta\nu\,\sin\nu_i + \cos\Delta\nu - 1\right)}{\sin\Delta\nu} \tag{21}$$

Note that Eq. (21) is free of singularity at $\Delta\nu = 0$ since, by assumption, $N \geq 3$, see Eq. (1). An explicit expression of $\widetilde{y}(\nu)$ and $\widetilde{y}'(\nu)$ in the i-th ballistic arc may now be obtained by substituting Eqs. (20) and (21) into Eqs. (16)–(17). The result is

$$\widetilde{y}(\nu) = \left[\frac{H\,\left(e\,\sin\Delta\nu\,\sin\nu_i + \cos\Delta\nu - 1\right)}{\sin\Delta\nu}\right]\,\sin\left(\nu - \nu_i\right) - H\,\left(1 + e\,\cos\nu_i\right)\,\cos\left(\nu - \nu_i\right) \tag{22}$$

$$\widetilde{y}'(\nu) = \left[\frac{H\,\left(e\,\sin\Delta\nu\,\sin\nu_i + \cos\Delta\nu - 1\right)}{\sin\Delta\nu}\right]\,\cos\left(\nu - \nu_i\right) + H\,\left(1 + e\,\cos\nu_i\right)\,\sin\left(\nu - \nu_i\right) \tag{23}$$

and the value of $\widetilde{y}'(\nu)$ at the end of the i-th ballistic arc reduces to

$$\widetilde{y}'(\nu_i + \Delta\nu) = \frac{H\,\left[2 - 2\,\cos\Delta\nu + e\,\cos\nu_i - e\,\cos(2\,\Delta\nu + \nu_i)\right]}{2\,\sin\Delta\nu} \tag{24}$$

The spacecraft velocity vector $\boldsymbol{v}_{s_i}$ (or $\boldsymbol{v}_{e_i}$) relative to B at the start (or end) of the i-th ballistic arc is obtained from Eq. (13) as

$$\boldsymbol{v}_{s_i} = k^2\,\left[e\,\widetilde{y}(\nu_i)\,\sin\nu_i + (1 + e\,\cos\nu_i)\,\widetilde{y}'(\nu_i)\right]\,\hat{\boldsymbol{j}} \tag{25}$$

$$\boldsymbol{v}_{e_i} = k^2\,\left[e\,\widetilde{y}(\nu_i + \Delta\nu)\,\sin(\nu_i + \Delta\nu) + (1 + e\,\cos(\nu_i + \Delta\nu))\,\widetilde{y}'(\nu_i + \Delta\nu)\right]\,\hat{\boldsymbol{j}} \tag{26}$$

Using Eqs. (20)–(21) and (24), the last two relations reduce to the compact form

$$\boldsymbol{v}_{s_i} = k^2\,H\,\frac{(\cos\Delta\nu - 1)\,(1 + e\,\cos\nu_i)}{\sin\Delta\nu}\,\hat{\boldsymbol{j}} \tag{27}$$

$$\boldsymbol{v}_{e_i} = k^2\,H\,\frac{2 - 2\,\cos\Delta\nu + 2\,e\,\cos(\nu_i + \Delta\nu) - e\,\cos\nu_i - e\,\cos(\nu_i + 2\,\Delta\nu)}{2\,\sin\Delta\nu}\,\hat{\boldsymbol{j}} \tag{28}$$

Equations (27) and (28) are the starting point for calculating the total velocity variation per revolution Δv, in an N-impulse maneuver, necessary for a CPO to approximate a given DNKO.

Total velocity variation analysis

At the end of $(i-1)$-th ballistic arc, when the spacecraft is at point P_i and its position in the inertial frame is given by Eq. (2), an impulsive maneuver removes the discontinuity in the velocity and the vehicle is immediately inserted into the succeeding i-th arc, see Fig. 2. The velocity variation Δv_i at P_i is

$$\Delta v_i = \|\boldsymbol{v}_{s_i} - \boldsymbol{v}_{e_{(i-1)}}\| \tag{29}$$

where $\boldsymbol{v}_{s_i}$ is given by Eq. (27), while $\boldsymbol{v}_{e_{(i-1)}}$ is the spacecraft velocity vector relative to B at the end of $(i-1)$-th ballistic arc. An expression for $\boldsymbol{v}_{e_{(i-1)}}$ is obtained from Eq. (28) by formally substituting ν_i with $\nu_{(i-1)} \equiv (\nu_i - \Delta\nu)$. After some simplification, the result is

$$\boldsymbol{v}_{e_{(i-1)}} = k^2\,H\,\frac{(1 - \cos\Delta\nu)\,(1 + e\,\cos\nu_i)}{\sin\Delta\nu}\,\hat{\boldsymbol{j}} \tag{30}$$

Substituting Eqs. (27) and (30) into Eq. (29), the expression of Δv_i becomes

$$\Delta v_i = 2\,k^2\,H\,\frac{(1 - \cos\Delta\nu)}{\sin\Delta\nu}\,(1 + e\,\cos\nu_i) \tag{31}$$

so that the total velocity variation per revolution can be written as a sum of Δv_i, viz.

$$\Delta v = \sum_{i=1}^{N}\Delta v_i = 2\,k^2\,H\,\frac{(1 - \cos\Delta\nu)}{\sin\Delta\nu}\,\left(N + e\,\sum_{i=1}^{N}\cos\nu_i\right) \tag{32}$$

Recalling that $N \geq 3$, from Eq. (1) the summation in Eq. (32) is [15]

$$\sum_{i=1}^{N} \cos \nu_i = \sum_{i=1}^{N} \cos\left(\frac{2\,\pi\,(i-1)}{N}\right) = 0 \tag{33}$$

and, therefore, Eq. (32) becomes

$$\Delta v = 2\,N\,k^2\,H\,\frac{(1-\cos\Delta\nu)}{\sin\Delta\nu} \qquad \text{with} \qquad \Delta\nu = \frac{2\,\pi}{N} \tag{34}$$

In particular, in the limit as $N \to \infty$, Eq. (34) reduces to the very compact expression

$$\lim_{N\to\infty} \Delta v = \Delta v_c \triangleq 2\,\pi\,k^2\,H = 2\,\pi\,H\,\sqrt{\frac{\mu}{p^3}} \tag{35}$$

where Δv_c is the total velocity variation per revolution in the continuous-thrust case. Notably, Δv_c depends on the orbital shape through the semilatus rectum only and, as such, it is not explicitly dependent on the orbital eccentricity. The previous equation generalizes the result obtained by Spilker [12] for a circular orbit of radius R, that is, $\Delta v_c = 2\,\pi\,H\,\sqrt{\mu/R^3}$.

In the special case of circular orbit, Eqs. (31) and (34) give also the interesting result

$$\Delta v_i = \frac{\Delta v}{N} = 2\,k^2\,H\,\frac{(1-\cos\Delta\nu)}{\sin\Delta\nu} \qquad \text{if} \quad e = 0 \tag{36}$$

which states that Δv_i takes the same value for all impulses, due to the cylindric symmetry of the problem. In an elliptic orbit such a symmetry is lost and, indeed, Δv_i is maximum at P_1 (pericenter) and minimum when P_i is near the apocenter (when $\cos\nu_i$ is minimum and negative), see Eq. (31). Finally, recalling Eq. (1), Eqs. (34) and (35) may be combined to obtain the dimensionless total velocity variation per revolution around the primary as

$$\frac{\Delta v}{\Delta v_c} = \frac{N\,[1-\cos(2\,\pi/N)]}{\pi\,\sin(2\,\pi/N)} \tag{37}$$

Note that the ratio $\Delta v/\Delta v_c$ depends on the number of impulsive maneuvers only, whereas the DNKO characteristics, that is, its semilatus rectum and displacement, are included in the expression of Δv_c given by Eq. (35). Therefore, under the assumption of azimuthally equally spaced (impulsive) maneuvers, the total Δv in the elliptic case can be obtained by considering a virtual, circular, DNKO with the same displacement as the original orbit, and a radius equal to the semilatus rectum of the actual reference orbit. Figure 3 shows the variation of $\Delta v/\Delta v_c$ with N. Note that $\Delta v/\Delta v_c < 5\%$ when $N \geq 9$, and $\Delta v/\Delta v_c < 1\%$ when $N \geq 19$. Accordingly, it may be concluded that an accurate approximation of an elliptic DNKO, in terms of total velocity variation per revolution, is possible using a CPO with about ten equally spaced maneuvers.

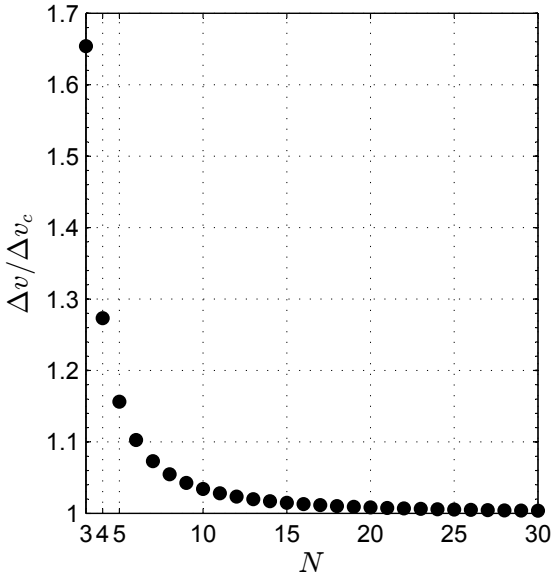

Figure 3 Dimensionless velocity variation $\Delta v/\Delta v_c$ as a function of N, see Eq. (37).

Model validation and mission application

The previous mathematical model has been validated through results taken from the literature [13] and by simulation, using the spacecraft nonlinear equations of motion.

Consider first a displaced geostationary orbit ($e = 0$), which is the same example as that discussed in Ref. [13]. Assuming a continuous thrust and observing that $\sqrt{\mu_\oplus/p^3} = 2\pi/(1\,\text{day})$, the velocity variation per revolution is, from Eq. (35)

$$\Delta v_c = \frac{4\,\pi^2\,H}{1\,\text{day}} \tag{38}$$

Let the displacement be $H = 35\,\mathrm{km}$ and $N = 10$. From Eq. (38) $\Delta v_c = 15.99\,\mathrm{m/s}$, whereas Eq. (37) gives $\Delta v/\Delta v_c \simeq 1.03425$, so that $\Delta v = 16.54\,\mathrm{m/s}$. In this case the velocity variation of the i-th maneuver is simply $\Delta v_i = \Delta v/N = 1.654\,\mathrm{m/s}$, according to Eq. (31). These values coincide with the results discussed in section 4 of Ref. [13]. Finally, the function $y = y(\nu)$ in the generic i-th ballistic arc can be obtained from Eq. (22) as

$$y(\nu) \equiv \widetilde{y}(\nu) = \frac{H\,[\cos(2\,\pi/N) - 1]}{\sin(2\,\pi/N)}\,\sin(\nu - \nu_i) - H\,\cos(\nu - \nu_i) \tag{39}$$

whose maximum modulus is obtained when $\nu = \nu_i + \Delta\nu/2 \equiv \nu_i + \pi/N$, viz.

$$|y|_{\max} = \frac{H}{\cos(\pi/N)} \simeq 36.8\,\mathrm{km} \tag{40}$$

A second interesting application of the proposed mathematical model consists in the generation of a CPO above the dwarf planet Ceres, which could allow a spacecraft to observe the polar zones of the celestial body. In this case the Keplerian reference trajectory is a heliocentric orbit ($\mu = \mu_\odot$), with eccentricity $e = 0.079$ and semilatus rectum $p = 2.7477\,\mathrm{au}$. Assuming a displacement $H = 80000\,\mathrm{km}$, the continuous thrust case requires a velocity variation per revolution (around the Sun) of about $\Delta v_c = 21.972\,\mathrm{m/s}$. Using $N = 10$ impulses, Eq. (34) gives $\Delta v \simeq 22.724$ with, again, $\Delta v/\Delta v_c \simeq 1.03425$. These results may be compared with those found by solving a series of targeting problems using the spacecraft nonlinear equations of motion in an inertial reference frame, where $(\hat{\boldsymbol{\imath}}_I, \hat{\boldsymbol{\jmath}}_I)$ coincides with the orbital plane of Ceres. The components of the velocity variation required in the i-th maneuver are reported in Tab. 1 along with those obtained from Eq. (31).

Table 1 Ceres mission case: components of $\Delta\boldsymbol{v}_i$ (m/s) obtained by numerical simulation.

Point	$\Delta\boldsymbol{v}_i \cdot \hat{\boldsymbol{\imath}} \times 10^5$	$\Delta\boldsymbol{v}_i \cdot \hat{\boldsymbol{\jmath}}$	$\Delta\boldsymbol{v}_i \cdot \hat{\boldsymbol{k}} \times 10^3$	Δv_i by Eq. (31)
P_1	0	−2.4520	0.7255	2.4520
P_2	0.2077	−2.4177	0.7054	2.4177
P_3	0.3235	−2.3280	0.6541	2.3280
P_4	0.3079	−2.2170	0.5935	2.2170
P_5	0.1825	−2.1272	0.5465	2.1272
P_6	0	−2.0930	0.5291	2.0930
P_7	−0.1825	−2.1272	0.5465	2.1272
P_8	−0.3079	−2.2170	0.5935	2.2170
P_9	−0.3235	−2.3280	0.6541	2.3280
P_{10}	−0.2077	−2.4177	0.7054	2.4177

Unlike the linear model, according to which the velocity variation vector is parallel to $\hat{\boldsymbol{\jmath}}$, the actual $\Delta\boldsymbol{v}_i$ has a nonzero component in the $\mathcal{P}$ plane. This component is however several order of magnitude smaller than that along $\hat{\boldsymbol{\jmath}}$ and, therefore, the value of Δv_i given by Eq. (31) and reported in the last column of Tab. 1, is an accurate approximation of the actual velocity variation required by the i-th maneuver. This conclusion is further confirmed by the total velocity variation per revolution, since $\sum_{i=1}^{N} \|\Delta\boldsymbol{v}_i\| \simeq 22.725\,\mathrm{m/s}$ nearly coincides with the value obtained from Eq. (34). Table 1 also shows a symmetry of the results with respect to the point P_6, which coincides with the orbit aphelion. Finally, the small differences of $\|\Delta\boldsymbol{v}_i\|$ at different points are due to the small value of the reference orbit eccentricity.

The last example is a CPO over the Mercury's poles. In this case $e = 0.2056$ and $p = 0.3707\,\mathrm{au}$, whereas the velocity variation per revolution (around the Sun), given by Eq. (34), is drawn in Fig. 4 as a function of $H \in [110,\,250] \times 10^3\,\mathrm{km}$ and $N = \{3, 4, 5, 10\}$. In particular, the figure confirms that a CPO generated by $N = 10$ equally spaced impulses requires a velocity variation per revolution close to Δv_c. Assuming, for example, $N = 10$ and $H = 150000\,\mathrm{km}$, the velocity variations are $\Delta v \simeq 0.8598\,\mathrm{km/s}$ and $\Delta v_c \simeq 0.8313\,\mathrm{km/s}$, while the values of Δv_i are shown in Fig. 5. In this case the non-negligible orbital eccentricity induces a marked Δv_i variation along the orbit.

Conclusions

An elliptic displaced orbit may be suitably approximated by a set of ballistic arcs patched by impulsive maneuvers, which take place at azimuthally equally spaced points. The use of Hill-Clohessy-Wiltshire equations allows the required velocity variation per revolution to be obtained at linear order with a compact and closed-form solution. The total velocity variation depends on the orbital displacement, is a function of the semilatus rectum of the displaced orbit and of the number of impulses but, notably, has not an explicit dependence on the orbital eccentricity. The special case of continuous thrust is obtained in the limit as the number of impulses tends to infinity, thus extending similar results available in the literature in the special case of circular orbit. The proposed mathematical model may be used in a more general set-up, when the impulses are applied at generic points along the orbit. Although in that case a compact solution for the total velocity variation per revolution is lost, the required velocity variation at any maneuver point is given analytically, and so an estimate of the mission performance can be obtained with a reduced computational cost.

References

[1] McInnes, C. R., "Dynamics, stability, and control of displaced non-Keplerian orbits," *Journal of Guidance, Control, and Dynamics*, Vol. 21, No. 5, 1998, pp. 799–805. doi: 10.2514/2.4309.

[2] McKay, R. J., Macdonald, M., Biggs, J. D., and McInnes, C. R., "Survey of Highly Non-Keplerian Orbits with Low-Thrust Propulsion," *Journal of Guidance, Control, and Dynamics*, Vol. 34, No. 3, 2011, pp. 645–666. doi: 10.2514/1.52133.

[3] Forward, R. L., "Light Levitated Geostationary Cylindrical Orbits," *Journal of the Astronautical Sciences*, Vol. 29, No. 1, 1981, pp. 73–80.

[4] Forward, R. L., "Light-Levitated Geostationary Cylindrical Orbits Using Perforated Light Sails," *Journal of the Astronautical Sciences*, Vol. 32, April-June 1984, pp. 221–226.

[5] Forward, R. L., "Light-levitated geostationary cylindrical orbits. Correction and expansion," *Journal of the Astronautical Sciences*, Vol. 38, No. 3, 1990, pp. 335–353.

[6] Simo, J. and McInnes, C. R., "Asymptotic Analysis of Displaced Lunar Orbits," *Journal of Guidance, Control, and Dynamics*, Vol. 32, No. 5, 2009, pp. 1666–1671. doi: 10.2514/1.43703.

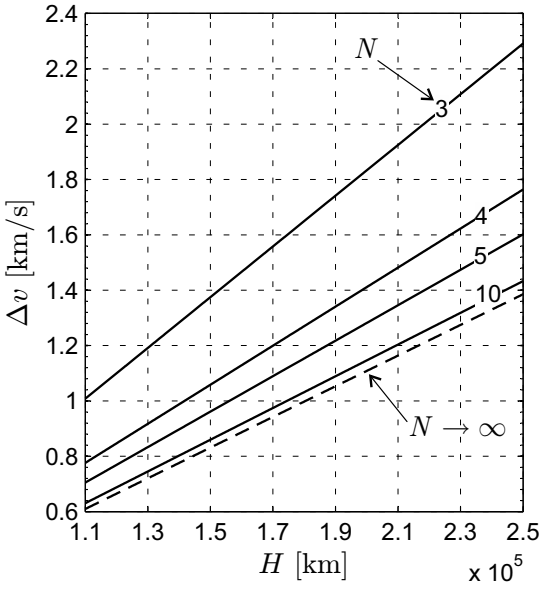

Figure 4 Mercury mission scenario: $\Delta v = \Delta v(N, H)$.

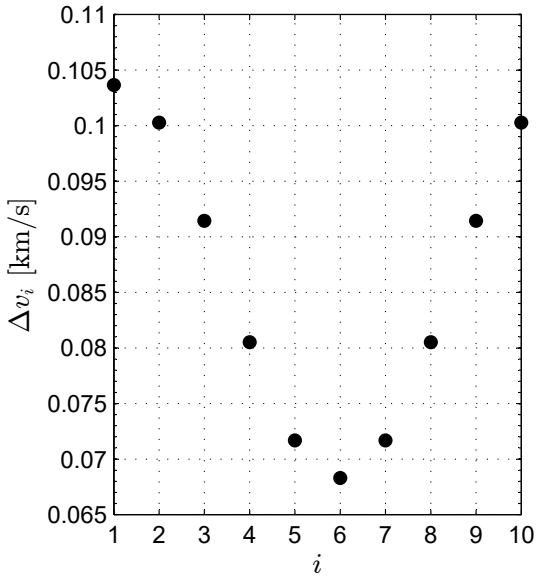

Figure 5 Mercury mission scenario: velocity variation in the i-th maneuver ($N = 10$ and $H = 150000\,\mathrm{km}$).

[7] Simo, J. and McInnes, C. R., "Designing Displaced Lunar Orbits Using Low-Thrust Propulsion," *Journal of Guidance, Control, and Dynamics*, Vol. 33, No. 1, 2010, pp. 259–265. doi: 10.2514/1.45305.

[8] Heiligers, J., Ceriotti, M., McInnes, C. R., and Biggs, J. D., "Displaced Geostationary Orbit Design Using Hybrid Sail Propulsion," *Journal of Guidance, Control, and Dynamics*, Vol. 34, No. 6, 2011, pp. 1852–1866. doi: 10.2514/1.53807.

[9] Gong, S. and Li, J., "Solar Sail Heliocentric Elliptic Displaced Orbits," *Journal of Guidance, Control, and Dynamics*, Vol. 37, No. 6, 2014, pp. 2021–2026. doi: 10.2514/1.G000660.

[10] Wang, W., Yuan, J., Mengali, G., and Quarta, A. A., "Invariant Manifold and Bounds of Relative Motion Between Heliocentric Displaced Orbits," *Journal of Guidance, Control, and Dynamics*, Vol. 39, No. 8, 2016, pp. 1764–1776. doi: 10.2514/1.G001751.

[11] Yashko, G. J. and Hastings, D. E., "Analysis of Thruster Requirements and Capabilities for Local Satellite Clusters," *10th Annual AIAA/USU Conference on Small Satellites*, Utah State University (Logan UT), Sept. 1996, Retrieved at `https://digitalcommons.usu.edu/smallsat/1996/all1996/49/` on June 14, 2018.

[12] Spilker, T. R., "Saturn ring observer," *Acta Astronautica*, Vol. 52, No. 2-6, Jan. 2003, pp. 259–265. doi: 10.1016/S0094-5765(02)00165-0.

[13] McInnes, C. R., "Displaced non-Keplerian orbits using impulsive thrust," *Celestial Mechanics and Dynamical Astronomy*, Vol. 110, No. 3, July 2011, pp. 199–215. doi: 10.1007/s10569-011-9351-5.

[14] Yamanaka, K. and Ankersen, F., "New State Transition Matrix for Relative Motion on an Arbitrary Elliptical Orbit," *Journal of Guidance, Control, and Dynamics*, Vol. 25, No. 1, 2002, pp. 60–66. doi: 10.2514/2.4875.

[15] Huo, M., Mengali, G., and Quarta, A. A., "Electric Sail Thrust Model from a Geometrical Perspective," *Journal of Guidance, Control and Dynamics*, Vol. 41, No. 3, 2018, pp. 735–741. doi: 10.2514/1.G003169.